International Journal of Current Engineering and Technology
E-ISSN 2277 – 4106, P-ISSN 2347 – 5161

Available at http://inpressco.com/category/ijcet

Research Article

Modulating Mathematical Model to Investigate Doublet Magnetic Lens

Ali Hadi-Al. Batat†, Hussain S. Hasan‡, Saadi Raheem Abbas†* and Mohammed Jawad Yaseen†

†Department of Physics, College of Education, the University of Mustansiriyah, P.O.Box: 46219, Baghdad, Iraq
‡Department of Physiology and Medical Physics, College of Medicine, Al-Nahrain University, P.O. Box: 70044, Kadhimiya, Baghdad, Iraq

Accepted 04 Aug 2016, Available online 05 Aug 2016, **Vol.6, No.4 (Aug 2016)**

Abstract

In the current research a new mathematical target function has been introduced to represent the field distribution of the doublet magnetic electron lens. As a common point of view, doublet magnetic electron lenses used in electron optical device to obtain rotation and distortion free images in the first and/or second loop. Design of this instrument has been investigated under the effect of the half half-width for the field distribution which is considered as a main effective optimization parameter including in the target function. Different values of this parameter have been chosen to simulate the electron optical device under some constraints and transformations. Rotation and radial distortion free doublet lens has been achieved. Also, rotation and distortion (radial and spiral) free images may be obtained at a very specific value of the optimization parameter taken under considerations.

Keywords*: Electron optics, Doublet Magnetic Lenses, Projector properties, Distortion.*

1. Introduction

The electromagnetic fields play an important role for controlling beams of charged particles concerning the acceleration, focusing, guidance, and deflecting. So, electron and ion optics arise as the theory and practice of production, control and utilization of the charged particle beams. The electron lens is defined as an instrument which collects a moving beam of charged particles or focuses them to the same point. Therefore, the action of electron lenses on an electron (or any charged particle) beam is a close analogy to that of convex glass lenses or eye on ray of visible light passing through it (H. H. Rose *et al*, 2009) .The properties of the final projector lens in an electron microscope column are very important. Usually, the accelerated electron beam will enter the final projector lens parallel to the optical axis. So, the infinite magnification mode will be introduced in this study. In general, the projector magnetic lenses suffer from several distortions like the radial and spiral distortions (J. Orloff *et al,* 2009).

The fourth kind of magnetic lenses can be obtained by coupling two double pole-piece magnetic lenses back to back having the same optical axis. Thus, these lenses consist of two-air gaps and usually called doublet lenses (S.M. Juma *et al*, 1975) or triple pole-piece lenses (K. Tsuno, Y. Harada *et al*, 1981), where the mid-plate that separate the two air-gaps is considered as a third pole piece. Doublet lenses have a distinct feature compared with other magnetic lenses due to its ability to provide rotation and distortion-free images when the currents supporting in the two gaps-width the same magnitudes and opposite directions.

2. Modulating mathematical model

A new mathematical field model has been suggested to represent a double pole-piece magnetic lens given by:

$$B_z(z)=\left[\frac{a^2}{\pi\left[(2z-a)^2+a^2\right]}\right] \quad (1)$$

Where **a,** is an optimization parameter which represents the half half-width of the field distribution. The gradient of the magnetic field distribution and its curvature can be evaluating analytically using the following equation.

$$B'_z(z)=\left[\frac{-4a^2(2z-a)}{\pi\left[(2z-a)^2+a^2\right]^2}\right] \quad (2)$$

$$B''_z(z)=\left(\frac{-8a^2}{\pi}\right)\left[\frac{1}{\left[(2z-a)^2+a^2\right]^2}-\frac{4(2z-a)^2}{\left[(2z-a)^2+a^2\right]^3}\right] \quad (3)$$

In the inverse design procedure, it is necessary to compute the axial magnetic scalar potential along the optical axis of the lens under considerations. However, by using Ampere's circuited law with aid of the equation ($\mathbf{B_z(z)=-\mu_0(dV_z/dz)}$), the trigonometric integral method can be used to integrate equation (1)

*Corresponding author: **Saadi Raheem Abbas**

along the optical axis to obtain the axial magnetic scalar potential distribution at each axial coordinate **z**, the result will be as follows;

$$V(z)=-\left(\frac{a}{2\mu_o\pi}\right)arctan\left(\frac{(2z-a)}{a}\right)\Bigg]_{z_s}^{z_f} \quad (4)$$

Where $\mathbf{z_s}$, and $\mathbf{z_f}$, are the terminals of the magnetic lens field, $\boldsymbol{\mu_o}$ is the permeability of free space (4π x10^{-7}H/m). The second derivative of the axial magnetic scalar potential distribution can be determined analytically from the equation.

$$V''(z)=\left[\frac{B_z'(z)}{\mu_o}\right]=\left[\frac{-4a^2(2z-a)}{\mu_o\pi\left[(2z-a)^2+a^2\right]^2}\right] \quad (5)$$

In the present work the mathematical field formula given in equation (1) has been used to represent the magnetic field distribution of a doublet (triple pole-piece) lens. However, this field formula can be carried out in the negative values of **z**-axis as a first double pole-piece lens and that in the positive **z**-values for the second lens. The main optimization parameter **a** in each lens will be changed to obtain the required doublet lens.

3. Theoretical considerations

It is well known that the defects of charged particle devices such that the electron lens depend on the function of that device, however, the objective charged particle lenses suffer from two main aberrations namely; spherical and chromatic aberration, in contrast, the radial and spiral distortion are the two fundamental geometrical defects from which the projector charged particle lenses suffer. Since, the present investigation deals with design of doublet projector magnetic lenses, thus, the latter two defects of magnetic lenses can be determined from the following integrals (S.I. Monokovosky and A.D. Sushkov *et al*, 2005; Hussian. S. Hasan, Mohammed Jawad Yaseen *et al,* 2015).

$$D_r=\left(\frac{\eta}{128V_r}\right)\int_{z_1}^{z_2}\left[\left(\frac{3\eta}{V_r}B_z^2+8B_z'^2\right)r_\alpha r_\gamma^3-4B_z^2(r_\gamma'^2r_\alpha r_\gamma+r_\gamma'\,r_\alpha^2r_\alpha')\right]dz \quad (6)$$

$$D_S=\int_{z_1}^{z_2}\left[\frac{3}{128}\left(\frac{\eta}{V_r}\right)^{3/2}r_\alpha^2B_z^3+\frac{1}{16}\left(\frac{\eta}{V_r}\right)^{1/2}r_\alpha'^2B_z\right]dz \quad (7)$$

Where r_α and r_γ are the two linearly independent solutions of the paraxial ray equation and the limits of integration are the two terminals coordinates $\mathbf{z_1}$ and $\mathbf{z_2}$ of the axial magnetic field distribution. However, the trajectory of the charged particle (electron in the case of magnetic lens) inside a rotationally symmetric magnetic field can be controlled by the paraxial ray equation which is a second-order, linear, homogenous ordinary differential equation given by (A.B. El-Kareh, J.C.J. El-Kareh *et al,* 1970).

$$r''+\frac{\eta}{8V_r}B_z^2(z)r=0 \quad (8)$$

Where η is the mass to the charge ratio of the electron respectively, and V_r is defined as the corrected relativistically accelerating voltage which is given by (O. Klemprer *et al*, 1971).

$$V_r=V_a\,(1+\,e\,V_a\,/2m\,c^2)=V_a\,(1+\,0.978x10^{-6}\,V_a) \quad (9)$$

Where V_a is the applied accelerating voltage. To obtain the electron beam trajectory inside the electron optical device (the magnetic lens in the present investigation) the paraxial ray equation can be solved analytically or numerically according to the constraints imposed in the study. However, the numerical Fourth-Order Runge-Kutta method has been used to solve paraxial ray equation under some constraints. By using the analytical solution of Laplace's equation, the shape of the pole-piece that would produce the desired magnetic field can be determined. Therefore, for an axially symmetric systems the electrostatic or magnetic scalar potential distribution $V(R_P,z)$ in the plane can be calculated from the axial distribution of the same potential V(z) by the following power series expansion (M. Szilagyi *et al*,1984).

$$V(R_p,z)=\sum_{k=0}^{\infty}\frac{(-1)^k}{(k!)^2}\left(\frac{R_p}{2}\right)^{2k}\frac{d^{2k}V(z)}{dz^{2k}} \quad (10)$$

Where R_p is the radial height of the pole-piece, V_P is the potential value at the pole-piece surface, which is equivalent to half of the lens excitation NI in the case of symmetrical charged particle lens, and V(z) is the second derivative of the magnetic scalar potential with respect to the **z**-coordinate. By taking the first two terms of equation (10) the equipotential surfaces (i.e. the magnetic pole-piece) can be determined from the following formula (M.J. Yaseen *et al*, 2013).

$$R_P(z)=2\left[\frac{V(z)-V_P}{V''(z)}\right]^{\frac{1}{2}} \quad (11)$$

4. Results and discussion

In the present work the effect of the optimization parameter **a** on the design of symmetrical doublet magnetic electron lenses and consequently the first order properties as well as third-order aberration has been taken under consideration. In addition a rotation and distortion-free doublet lens has been carried out. However, it should be mentioned that the optical properties and the lens configuration are not affected by changing the length of the lens.

5. Single magnetic lens

To study the effect of the optimization parameter **a,** the following five values of **a** are selected (1, 2, 3, 4, and

5mm). To be the lens operates under the magnetic unsaturated mode, the length of the lens is kept constant at 100mm. From the suggested model equation, i.e., equation (1), it is noted that the distribution of the magnetic field will be shifted from the symmetry plane (i.e., z=0) by a distance approximately equals to the half half-width **a**, and consequently the distribution of the magnetic scalar potential as shown in figures 1. It should be mentioned that, this shift in the field and potential distributions makes these distributions are asymmetric about the symmetry plane. Therefore, some axial transformations have been carried out to make these distributions symmetric around the symmetry plane (z=0) as shown in figure 2. However, figure 3, shows the half-width upper reconstructed magnetic pole-piece shape at **a**=1mm.

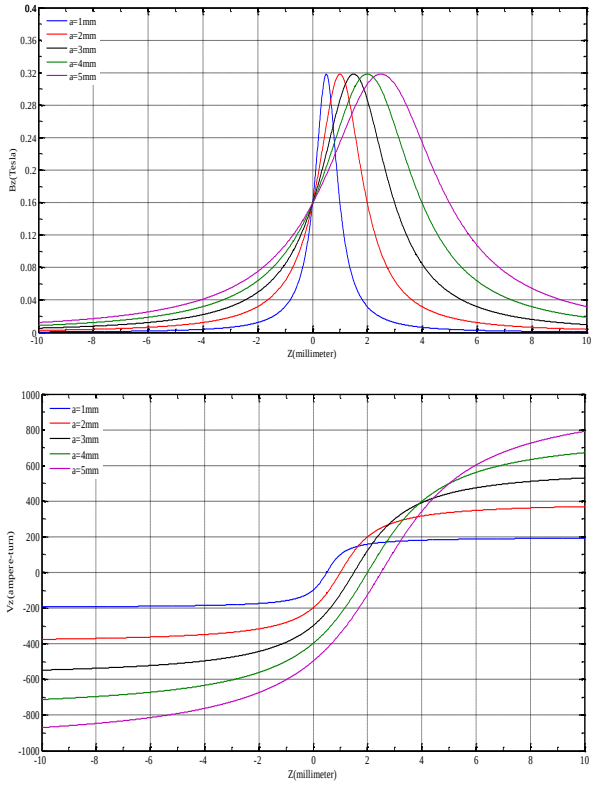

Figure 1: The shifted axial magnetic field and magnetic scalar potential distributions from the symmetry plane for different values of the parameter **a**

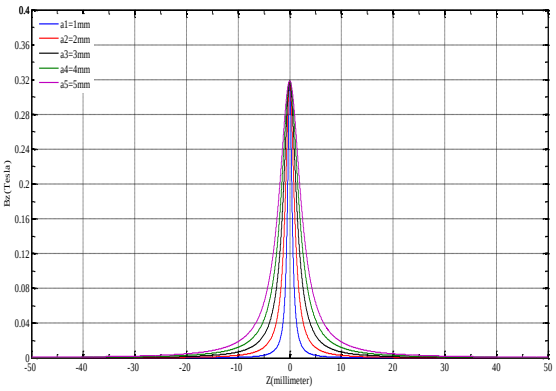

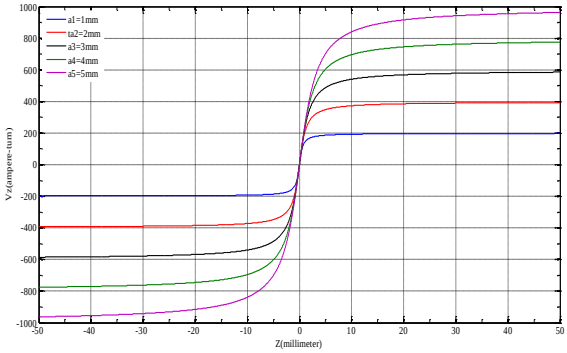

Figure 2: The symmetric axial magnetic field and magnetic scalar potential distributions around the symmetry plane for different values of the parameter **a**

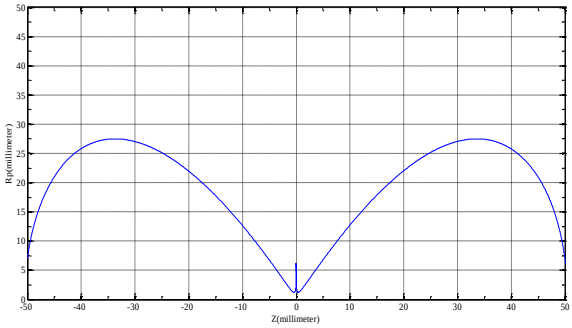

Figure 3: The half upper reconstructed magnetic pole-piece shape at **a**=1mm

The properties of the lens field $\mathbf{B_{max}}$(peak field), **W** (half-width of the field) and the excitation of the lens **NI** (area under the field curve) as the function of the different chosen values of the parameter **a** are shown in the figure 4. It is obvious that when the parameter **a**, is increasing the peak field value $\mathbf{B_{max}}$ of the corresponding fields is not affected. On other hand, the area under each field distribution **NI** and consequently the half-width **W** of the field are increased by increasing the parameter **a**. This means that the field distribution would be more distributed along a large axial extension_of the optical axis for large values of parameter **a**

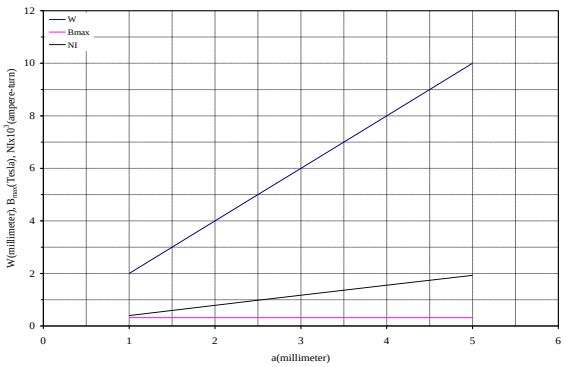

Figure 4: Variation of maximum value of the flux density $\mathbf{B_{max}}$,the half-width of the field W and area under the field curve or excitation **NI,** as a function of **a**

6. Doublet magnetic lens

With the aid of the suggested magnetic field mathematical model given in equation1, and using some axial transformations for the negative values of the optical axis $z_s \le z \le 0$ and positive values of the optical axis $0 \le z \le z_f$ the doublet or triple pole-piece magnetic lens can be obtained. The axial distribution functions of the first and the second lens of the doublet magnetic lens could be affected by the parameters $\mathbf{a_1}$ and $\mathbf{a_2}$ which can take identical values as those of the parameter **a** in the case of the single symmetrical double pole-piece magnetic lens. However, since the present work aims to investigate a rotation and distortion free doublet lenses, the length of each single lens of the doublet lens are chosen equal to 100mm. To obtain a rotation and distortion free doublet lens, one can calibrate the parameters $\mathbf{a_1}$ and $\mathbf{a_2}$ of the first and second field lenses to be the excitations of the two lenses are equal and opposite sign, .i.e. $\mathbf{NI_1=-NI_2}$. However, these parameters are changing until obtain a doublet lens design having spiral and radial distortion-free images. Therefore, the parameters of the first (left) lens are denoted by $\mathbf{NI_1}$ and $\mathbf{a_1}$, while those for the second (right) lens are denoted by $\mathbf{NI_2}$ and $\mathbf{a_2}$.

To study the effect of the parameter $\mathbf{a_2}$ on the design and the properties of the doublet lens, the parameter $\mathbf{a_1}$ of the first lens is kept constant at 1mm, accordingly the excitation of this lens $\mathbf{NI_1}$ remains fixed approximately at 200(ampere-turn). Thus, since $\mathbf{a_1}$ is kept constant and $\mathbf{NI_1}$ unchanged, this means that the field distribution of the first lens uncharged. Therefore, five values of the parameter $\mathbf{a_2}$ of the second lens have been chosen (1, 2, 3, 4, and 5mm) to investigate the properties and design of the doublet lens. However, according to these values of $\mathbf{a_2}$, figure5 shows the axial magnetic field distribution of the doublet lens at $\mathbf{a_1}$=1mm. The pole-piece profile of the doublet lens corresponding to the field distribution plotted in figure5 is shown in figure6.

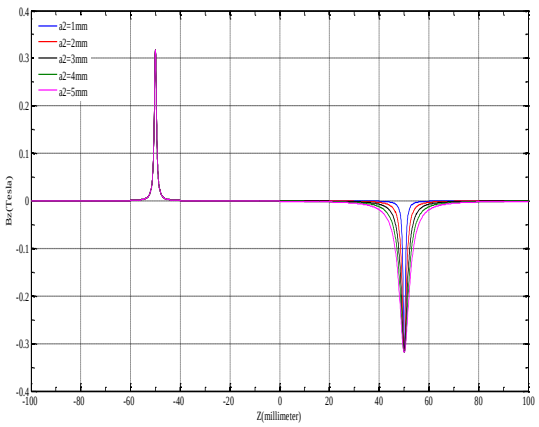

Figure 5: The axial magnetic field distribution along the optical axis of the doublet lens for different values of the parameter $\mathbf{a_2}$ when $\mathbf{a_1}$=1 mm

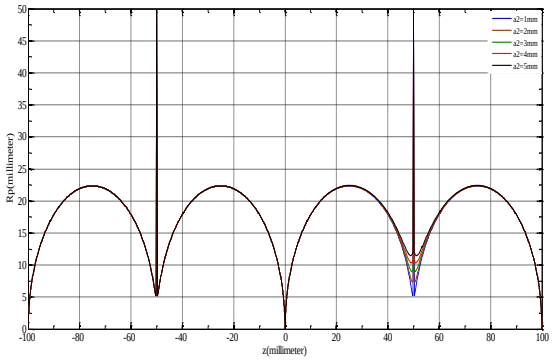

Figure 6: The half upper reconstructed pole shapes of the doublet lens for different values of $\mathbf{a_2}$, when $\mathbf{a_1}$=1 mm

Figure 7 shows the projector focal length $\mathbf{(F_p)}$ curves in the first loop of the doublet lens as a function of the excitation parameter $NI/V_r^{1/2}$. One can see from the figure that the excitation parameter for all values of $\mathbf{a_2}$ is confined in the interval $0.5 \le NI/V_r^{1/2} \le 3.0$ The minimum value of the projector focal length $\mathbf{(F_P)_{min}}$ when $\mathbf{a_2}$=1 mm is equal to the distance between the center of the two fields which is 100 mm, where in this operation the first and second lens are identical, this means that $\mathbf{F_{p1}=F_{p2}=\ell=(F_P)_{min1}}$ according to the relation (S.M. Juma *et al,*1975) .

$$F_p = \left(\frac{F_{p1} F_{p2}}{F_{p1} + F_{p2} - \ell} \right) \qquad (12)$$

Where $\boldsymbol{\ell}$ is distance between the lenses. Variation of $\mathbf{(F_P)_{min1}}$, and the magnification of the lens **M1** in first loop with the parameter $\mathbf{a_2}$ are shown in figure 8. It is noted that **M1** increasing with parameter $\mathbf{a_2}$, while $\mathbf{(F_P)_{min1}}$ decreasing with $\mathbf{a_2}$. This variation states that when the first and second lens are not identical the minimum value of the projector focal length is not equal to the distance between the centers of the two fields $\boldsymbol{\ell}$, see table 1. It is noted that in this table the values of $\mathbf{(F_P)_{min1}}$ are computed with the aid of equation 12, and compared with those evaluated in program.

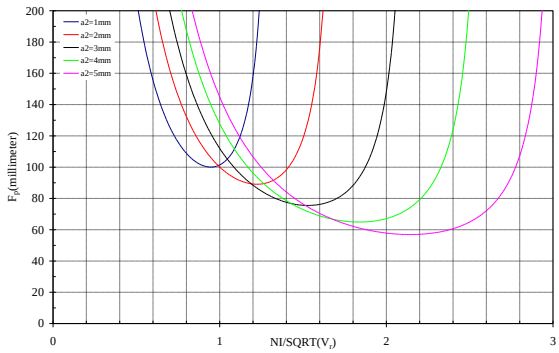

Figure 7: The projector focal length F_p as a function of $NI/V_r^{1/2}$ for different values of $\mathbf{a_2}$=(1, 2, 3, 4and 5mm)

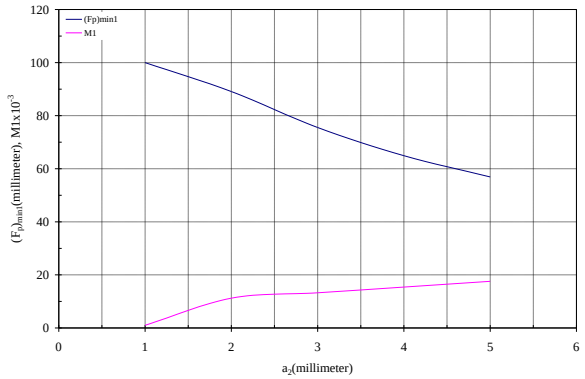

Figure 8: Variation of minimum value of the projector focal length $(F_p)_{min1}$, and magnification of lens **M1** as a function of a_2

Table 1: Some projector focal properties of the doublet lens in the first loop for various values of $\mathbf{a_2}$

NI/SQRT(V_r)			$(F_p)_{min1}$ (millimeter)		F_{p2}	F_{p1}	a_2
D_s=0	D_r=0	$(F_p)_{min1}$	Theoretical	Computed	millimeter	millimeter	millimeter
1.33	0.95	0.95	98.46	100	99.23	99.23	1
1.56	1.23	1.23	134.2	89.09	117.1	59.29	2
1.8	1.35	1.53	124.6	75.52	112.3	38.4	3
2.04	1.45	1.84	105	64.91	102.5	26.63	4
2.26	1.54	2.14	87.62	56.91	93.81	19.57	5

The radial distortion coefficient D_r in the first loop of the doublet lens as a function of $NI/V_r^{1/2}$ is shown in figure 9. It is noted that the radial distortion vanishes for all values of $\mathbf{a_2}$ approximately for $0.95 \le NI/V_r^{1/2} \le 1.54$, see table1.

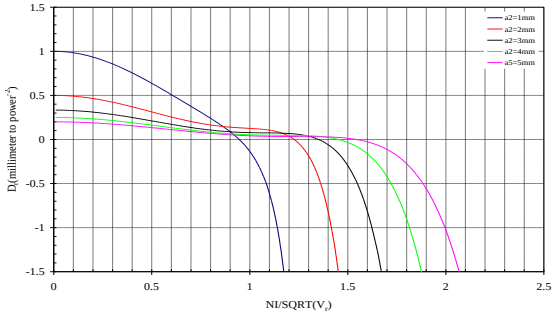

Figure 9: The radial distortion coefficient D_r of the doublet lens as a function of $NI/V_r^{1/2}$ for various values of $\mathbf{a_2}$

The spiral distortion coefficient $\mathbf{D_s}$ in the first loop of the doublet lens as a function of the excitation parameter $\mathbf{NI/V_r^{1/2}}$ for different values of $\mathbf{a_2}$ plotted in the figure 10. It is noted that for single lens, there is an increases in the conventional variation of $\mathbf{D_s}$ with $\mathbf{NI/V_r^{1/2}}$ especially at the high values of $\mathbf{NI/V_r^{1/2}}$, but for the doublet lens the coefficients $\mathbf{D_r}$, $\mathbf{D_s}$, and $\mathbf{F_p}$ have two loops. Although, the excitation parameter for all $\mathbf{a_2}$ values at which the parameter $\mathbf{D_s}$ vanishes differs in a very small shift from that in which the first magnification point occurs, but if the values of D_s coefficient are compared with those for the single lens, one can note that there is a very small difference. However, the values of the excitation parameter at which both radial and spiral distortions equal to zero are located at a limited small interval with respect to those at which the minimum focal length occurs. Therefore, the doublet magnetic lens of the parameters $\mathbf{a_1}$=1mm, $\mathbf{a_2}$=2mm, $\mathbf{NI_1}$=-$\mathbf{NI_2}$=200A-t has zero radial distortion at the first magnification point, i.e., at **NI**=1.23 A-t/(Volt)$^{1/2}$, also the value of the spiral distortion at this excitation parameter is very small which may be approximately equal to zero. However, this doublet lens may be considered as a rotation and distribution free electron optical device.

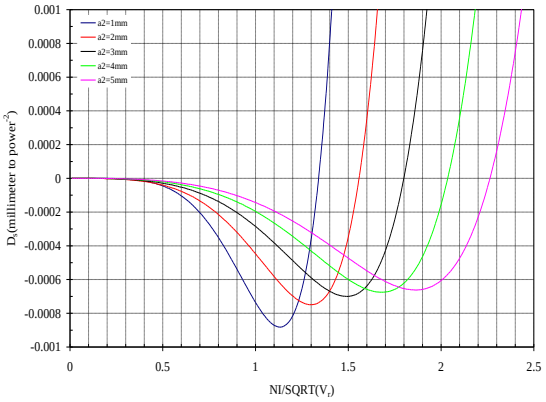

Figure 10: The spiral distortion coefficient D_s of the doublet lens as a function of $NI/V_r^{1/2}$ for different values of $\mathbf{a_2}$

Figure11 shows the variation of the projector focal length F_p in the second loop as a function of $NI/V_r^{1/2}$. It is noted that the minimum value of this parameter denoted by $(Fp)_{min2}$ increases (in the negative direction) with increasing $\mathbf{a_2}$, this means that the magnification in the second loop **M2** decreases with increasing $\mathbf{a_2}$ values, see figure 12.

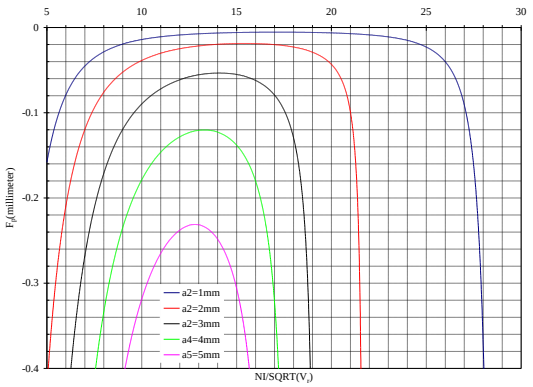

Figure 11: The projector focal length F_p as a function of $NI/V_r^{1/2}$ in the second loop for different values of $\mathbf{a_2}$

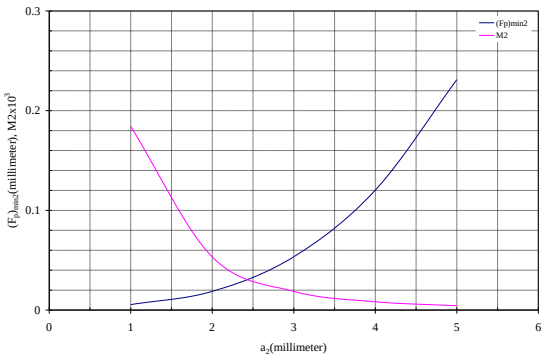

Figure12: Variation of the minimum value of the projector focal length $(F_p)_{min2}$, and magnification of lens **M2** as a function of a_2 at the second loop

Variation of the radial distortion coefficient D_r in the second loop as a function of the excitation parameter $NI/V_r^{1/2}$ is shown in figure 13. However, in spite of that the magnification decreases with increasing $\mathbf{a_2}$, but increasing of $\mathbf{a_2}$ makes the position of the second magnification point denoted by **M2** close to the point in which the radial distortion vanishes. In other words, one can see that as $\mathbf{a_2}$ increases the doublet lens in the second loop may give a radial distortion- free image in **M2**.

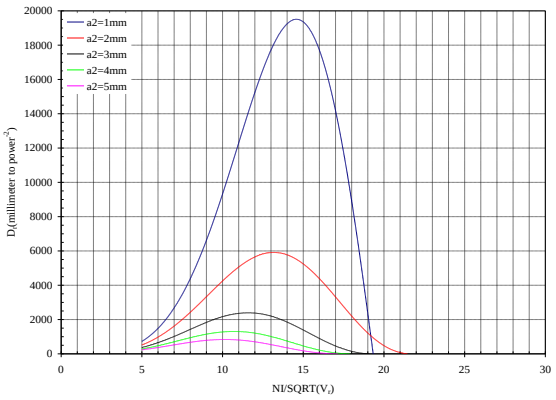

Figure 13: The radial distortion coefficient D_r with $NI/V_r^{1/2}$ in the second loop for different values of $\mathbf{a_2}$

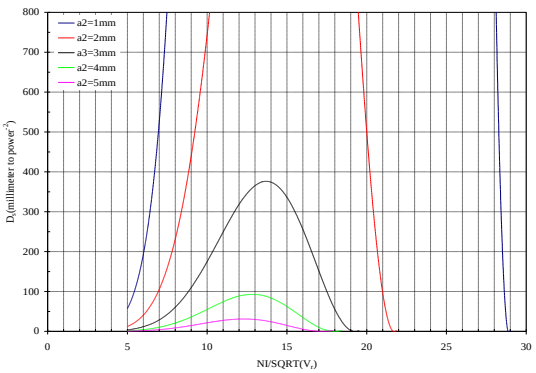

Figure 14: Variation of the spiral distortion D_s with $NI/V_r^{1/2}$ in the second loop for different values of $\mathbf{a_2}$=(1, 2, 3, 4, and 5mm)

Figure 14 shows the variation of the spiral distortion coefficient D_s in the second loop with the excitation parameter $NI/V_r^{1/2}$. It is well known in the current investigation that increasing of $\mathbf{a_2}$ gives an increasing in the air gap region and the bore radius of the second lens as shown in the reconstructed pole-pieces in figure 6. Therefore, the area under the D_s curve decreases with increasing $\mathbf{a_2}$. One can conclude that a spiral distortion free image can be obtained in the second loop for high values of $\mathbf{a_2}$, see table 2.

Table 2: Some projector focal properties of the doublet lens in the second loop for various values of $\mathbf{a_2}$

NI/SQRT(V_r)			$(F_p)_{min2}$	a_2
D_s=0	D_r=0	$(F_p)_{min2}$	(millimeter)	(millimeter)
17.1	16.95	17.15	-0.005427	1
17.84	17.73	15.42	-0.01872	2
19.15	18.98	14.08	-0.05346	3
21.65	21.4	13.3	-0.12003	4
28.86	19.33	12.81	-0.2311	5

Conclusions

The current study has been shown that a rotation and radial distortion free images formative in the constructed doublet electron lens can be obtained. Also, rotation and distortion free images can be procured at a specific value of the effective optimization parameter taken under considerations. However, the reason for the rear result may be owing to the structure mathematical field distribution model has no containing the excitation of the lens parameter **NI**.

References

H. H. Rose (2009), Geometrical Charged-Particle Optics, Springer Series in Optical Sciences.

J. Orloff (2009) Hand Book of Charged Particle Optics, second edition by Taylor and Francis group, CRC PRESS, London.

S.M. Juma (1975),Rotation Free Magnetic Electron Lenses,Ph.D. Thesis, University of Aston, Birmingham, England ,UK.

K. Tsuno, Y. Harada (1981), Elimination of Spiral Distortion in Electron Microscope Using an Asymmetric Triple-Pole Piece Lens, J. Phys. E: Sci. Inst., 14, 955-960.

S.I. Monokovosky and A.D. Sushkov,(2005)Intense Electron and Ion Beams, Printed in Germany , Springer-Verlag Berlin Heidel- Beg.

Hussian. S. Hasan, Mohammed Jawad Yaseen (2015) Image formation free rotation in triple pole-piece magnetic lenses, Journal of Advance in Physics Theories an d Applications,V(42), pp.46-55.

A.B. El-Kareh, J.C.J. El-Kareh (1970),Electron beams, lenses, and optics, (Academic Press).

O. Klemprer (1971), Electron Optics, 3rd ed., (Cambridge).

M. Szilagyi (1984),Reconstruction of Electrodes and Pole-pieces from Optimized Axial Field distributions of Electron and Ion optics Systems, Appl. Phys.Lett, V(45), pp.499-501.

M.J. Yaseen (2013). Projector Properties of the Magnetic Lens Depending on Some Physical and Geometrical Parameters, Journal of (IJAIEM),V(2), Issue 9, pp.195-202.